

## STABILITY OF MONTMORILLONITE EDGE FACES STUDIED USING FIRST-PRINCIPLES CALCULATIONS

HIROSHI SAKUMA<sup>1,\*</sup>, YUKIO TACHI<sup>2</sup>, KENJI YOTSUJI<sup>2</sup>, SHIGERU SUEHARA<sup>1</sup>, TATSUMI ARIMA<sup>3</sup>, NAOKI FUJII<sup>4</sup>, KATSUYUKI KAWAMURA<sup>5</sup>, AND AKIRA HONDA<sup>2</sup>

<sup>1</sup> National Institute for Materials Science, 1-1 Namiki, Tsukuba, Ibaraki 3050044, Japan

<sup>2</sup> Japan Atomic Energy Agency, 4-33, Muramatsu, Tokai-mura, Ibaraki, 3191194, Japan

<sup>3</sup> Kyushu University, 744, Motoooka, Nishi-ku, Fukuoka 8190395, Japan

<sup>4</sup> Radioactive Waste Management Funding and Research Center, 6-4 Akashicho, Chuo-ku, Tokyo 1040044, Japan

<sup>5</sup> Okayama University, 3-1-1, Tsushimanaka, Kita-ku, Okayama 7008530, Japan

**Abstract**—The reactivity and stability of the edge faces of swelling clay minerals can be altered by layer charge and the stacking structure; however, these effects are poorly understood due to experimental limitations. The structure and stability of the montmorillonite {110}, {010}, {100}, and {130} edge faces with a layer charge of either  $y = 0.50$  or  $y = 0.33$  ( $e^-/\text{Si}_4\text{O}_{10}$ ) were investigated using first-principles calculations based on density functional theory. Stacked- and single-layer models were tested and compared to understand the effect of stacking on the stability of montmorillonite edge faces. Most stacked layers stabilize the edge faces by creating hydrogen bonds between the layers; therefore, the surface energy of the layers in the stacked-layer model is lower than in the single-layer model. This indicates that the estimates of edge face surface energy should consider the swelling conditions. Negative surface energies were calculated for these edge faces in the presence of chemisorbed water molecules. A high layer charge of 0.50 reduced the surface energy relative to that of the low layer charge of 0.33. The isomorphic substitution of Mg for Al increased the stability of interlayer Na ion positions, which were stable in the trigonal ring next to the Mg ions. The lowest surface energies of the {010} and {130} edge faces were characterized by the presence of Mg ions on edge faces, which had a strong cation adsorption site due to the local negative charge of the edges. The coordination numbers of O atoms around cations adsorbed to these edge faces were small in comparison to interlayers without water.

**Key Words**—Chemisorbed Water Molecule, Clay, Density Functional Theory, Interlayer Bonding Energy, Isomorphic Substitution, Layer Charge, Single Layer, Smectite, Stacked Layer, Surface Energy.

### INTRODUCTION

Clay minerals have a layered structure and the stability is related to the interlayer bonding energy and surface energy of the edges and basal planes. The atomic structure of the interlayer space, the edges, and basal planes are, therefore, important factors in understanding and controlling mineral crystal growth and dissolution. The high affinity of clay mineral surfaces for cations and organic molecules has been noted in the recovery of toxic and radioactive materials from the environment (Welfare *et al.*, 1999; Tachi and Yotsuji, 2014). Clay minerals, thus, are used in oil recovery (He *et al.*, 2015; Mohammed and Babadagli, 2015) and chromatography (Lew *et al.*, 1946; Nakamura *et al.*, 1989; Yamagishi and Sato, 2012) and to prepare clay-polymer nanocomposites (Ray, 2014).

The structure of clay surfaces is also strongly correlated with the adsorbent properties. The atomic structure of adsorbent surfaces has been investigated using a combination of X-ray diffraction (XRD), nuclear

magnetic resonance (NMR), vibrational spectroscopy, and titration analysis. The XRD method is used to examine periodic systems; therefore, many studies have focused on the periodic interlayer structure of clay minerals (Ferrage *et al.*, 2005, 2010; Morodome *et al.*, 2011). Recent advances in X-ray surface scattering revealed the surface structure at muscovite/liquid interfaces (Cheng *et al.*, 2001; Schlegel *et al.*, 2006; Sakuma *et al.*, 2011; Lee *et al.*, 2012; Pinteá *et al.*, 2016). The X-ray surface scattering method, however, is limited to measuring the surface of large, single crystals, such as muscovite. Although the structures of the interlayer space and basal planes have been studied, the edge sites of clay minerals are poorly understood due to experimental limitations. These edge sites are particularly important, however, for small clay particles with large specific surface areas. Although NMR (Bowers *et al.*, 2008; Tansho *et al.*, 2016), X-ray absorption fine structure (XAFS) (Bostick *et al.*, 2002; Fan *et al.*, 2014), vibrational spectroscopy (Kubicki *et al.*, 1999), and titration (Tournassat *et al.*, 2004) analyses have revealed the local environments of adsorbent and clay surfaces, a structural model of the edge sites is still missing but is required to understand the results of these experimental methods.

\* E-mail address of corresponding author:

sakuma.hiroshi@nims.go.jp

DOI: 10.1346/CCMN.2017.064062

The edge structures of 2:1 dioctahedral clay minerals were examined (White and Zelazny, 1988) on the basis of a crystal growth theory (Hartman, 1973). The stable edges were estimated to occur on a parallel plane with continuous chains of strong bonds in the structure and a similar bulk composition. These edges were described as {110} and {010} faces assigned in a conventional unit cell of a *trans*-vacant (*C2/m*) montmorillonite (Tsipursky and Drits, 1984). Two other possible faces, {100} and {130}, have been observed in phlogopite synthesized using a hydrothermal method (Sun and Baronnet, 1989a; 1989b). The four {110}, {010}, {100}, and {130} edge faces were, therefore, considered in the present study as the plausible edge planes of 2:1 clay minerals.

The surface Coulomb energies of the {110}, {010}, {100}, and {130} edge faces were determined using simple electrostatic calculations for pyrophyllite (Bleam *et al.*, 1993). They selected pyrophyllite as a model 2:1 dioctahedral clay mineral because isomorphic substitutions are absent, which simplifies the variation in edge structures. Their work, however, assumed point charges, fixed atoms at the bulk unit-cell positions, and no tetrahedral tilting and neglected the van der Waals interaction, which resulted in many uncertainties in examining the stability of edge planes.

The relaxed structures of the pyrophyllite {110} and {010} edge faces were estimated using first-principles calculations based on density functional theory (DFT) (Bickmore *et al.*, 2003). This approach revealed realistic interatomic distances for the edges, which are useful for estimating the pKa values of the functional groups at the edge faces. Others (Churakov, 2006; Martins *et al.*, 2014; Newton and Sposito, 2015) evaluated the stability and reactivity of the pyrophyllite {010}, {110}, {100}, and {130} faces using DFT and classical molecular dynamics (MD) calculations. The dynamics of protonation and deprotonation reactions and adsorbed metal ions at some pyrophyllite edge faces have also been investigated using first-principles MD simulations (Churakov, 2007; Liu *et al.*, 2012b), including the adsorption of Cd(II) complexes (Zhang *et al.*, 2016). For simplicity, these pioneering works focused only on pyrophyllite, but they set the stage for investigation of more complex, isomorphically substituted systems.

Liu *et al.* (2012a) and Kremleva *et al.* (2015) examined the effects of isomorphic substitutions in the octahedral (Mg for Al) and tetrahedral (Al for Si) sheets on the atomic-scale structures and reactivity of the {010} and {110} faces using first-principles MD simulations. Values for pKa were recently estimated (Tazi *et al.*, 2012; Liu *et al.*, 2013, 2014) for clay minerals by using a combination of the vertical energy gap method and first-principles MD simulations. The pKa value of SiOH ( $6.8 \pm 0.4$ ) on the pyrophyllite {010} face can increase by 2–3 pKa units from isomorphic substitutions in the octahedral sites (Mg for Al) (Liu *et al.*, 2013). This finding implies that the layer charge can

alter the reactivity and stability of edge faces. The layer charge induced by isomorphic substitution in the aforementioned studies was fixed to 0.25 ( $e^-/\text{Si}_4\text{O}_{10}$ ), possibly due to the limited size of clay minerals in the simulation cell. The layer charge of swelling clay minerals ranges from 0.2 to 0.6; therefore, a wide range of layer charges should be examined for further discussion.

In a recent theoretical study using classical MD simulations and DFT simulations, Newton *et al.* (2016) evaluated the structure and stability of montmorillonite {110} edge planes with a layer charge of 0.40, 0.375, or 0.25 ( $e^-/\text{Si}_4\text{O}_{10}$ ) derived from stable Mg substitutions in the octahedral sheet. The increased layer charge due to Mg substitution yielded five-coordinate Mg ions at the edges. This type of structural change may explain the modeled sorption of U(VI) and Np(V) on a montmorillonite edge surface with a layer charge of 0.25 ( $e^-/\text{Si}_4\text{O}_{10}$ ) (Kremleva *et al.*, 2015; Kremleva and Krüger, 2016). In order to understand better the structure and stability of possible edge structures and the sorption of various cations onto these edge faces, further quantitative investigation of the surface energies of {110}, {010}, {100}, and {130} edge faces as a function of layer charge and Mg substitution is needed.

Molecular simulations are a powerful tool to understand clay mineral properties as was demonstrated in a recent special issue of *Clays and Clay Minerals* (Kalinichev *et al.*, 2016). The purpose of the present study was threefold: (1) to use the DFT method to model the surface energies of the {110}, {010}, {100}, and {130} edge faces of a single montmorillonite layer having a layer charge of 0.33 or 0.50 ( $e^-/\text{Si}_4\text{O}_{10}$ ), obtained by octahedral Mg substitution; (2) to determine the effects of layer charge and isomorphic substitution on the edge face stability; and (3) to apply the technique to stacked structures in order to calculate interlayer bonding energy, with an eye to developing the fundamental physics of clay mineral swelling.

## STRUCTURAL MODEL OF MONTMORILLONITE

Montmorillonite is a 2:1 dioctahedral smectite and Mg for Al octahedral isomorphic substitutions induce a negative layer charge, which is compensated by interlayer cations that connect the layers together. The layer charge magnitude can be determined from the amount of isomorphic substitutions using the following montmorillonite chemical formula:



where  $y$  is the interlayer charge ( $e^-/\text{Si}_4\text{O}_{10}$ ) that can range from 0.2 to 0.6,  $\text{M}^+$  is a monovalent interlayer cation, and  $n$  is the number of interlayer water molecules. The high computational cost of DFT calculations can be minimized by restricting the number of atoms in a periodic unit cell. The stability of the montmorillonite edge faces was

evaluated using a single layer in the unit cell. In this model, the periodic edge faces are described by the minimum of four octahedral sites is required to describe

periodic boundary conditions parallel to the edge faces. A minimum of four octahedral sites is required to describe

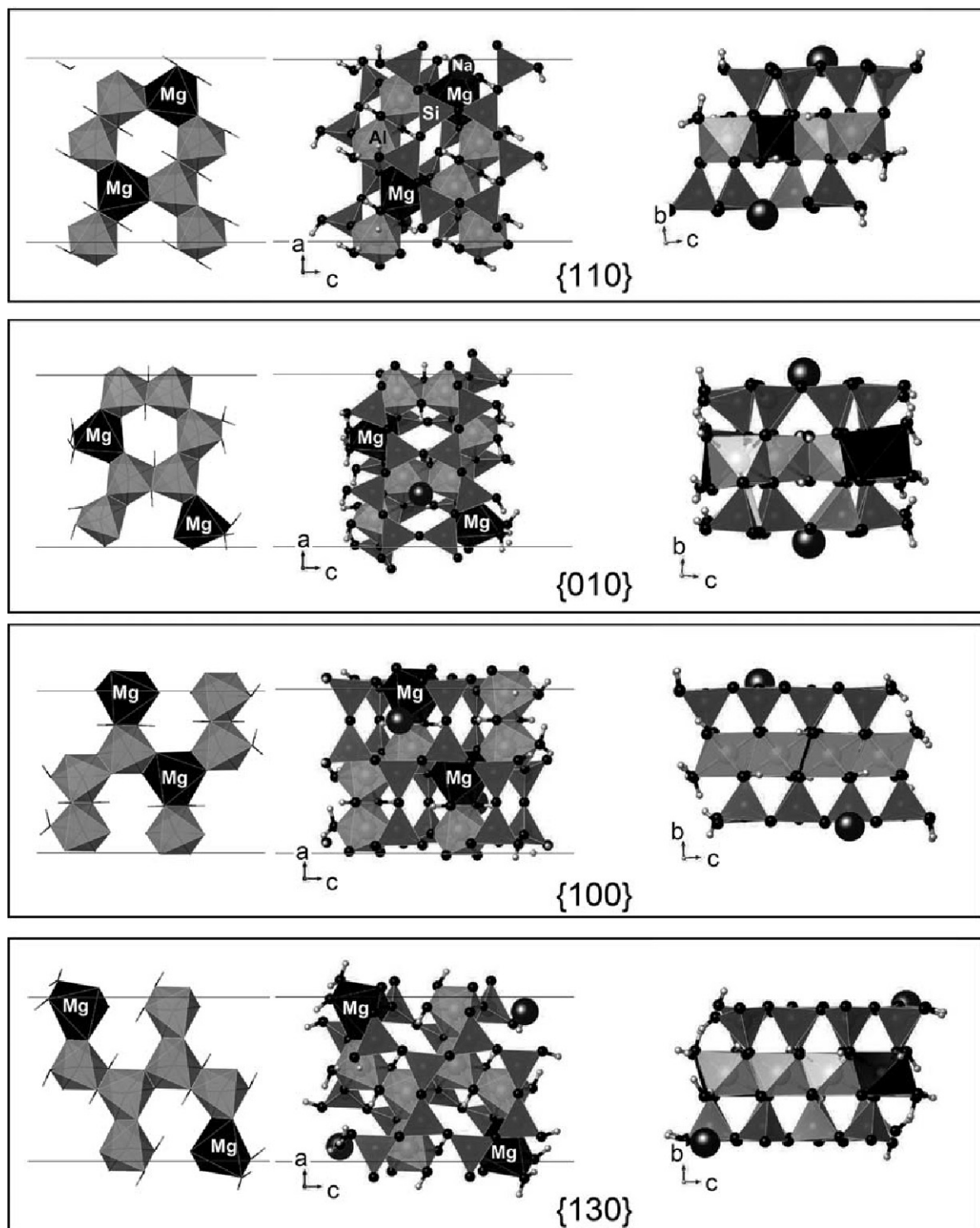


Figure 1. Top (center) and side (right) views of single-layer edge models for layer charge  $y = 0.50$ . The octahedral sheets are shown on the left to indicate the isomorphous substitution of Mg for Al. The edge faces are nearly parallel to the  $ab$  plane. The  $a$ ,  $b$ , and  $c$  axis values that were used to define the supercell were different than the montmorillonite axis parameters.

the  $\{100\}$  and  $\{130\}$  faces. The smallest number of unit cell atoms under this constraint depends on the layer charge ( $y$ ) and is 82 atoms for  $y = 0.50$  and 122 atoms for  $y = 0.33$ . To remove a dangling bond from the edge faces, four  $\text{H}_2\text{O}$  molecules were chemisorbed on both sides of the edge faces. To avoid an artifact that can arise from the periodic boundary conditions and the interactions between both sides of the edge faces, the unit cell length ( $a$ ) and the distance between the edge faces were taken to be

$>9 \text{ \AA}$ . The total number of atoms in the unit cell was 106 atoms for  $y = 0.50$  (Figure 1) and 146 atoms for  $y = 0.33$  (Figure 2). Various initial configurations for the Na and Mg ions were tested to obtain the energy differences, which depended on the ion positions. Two constraints were employed to avoid unstable configurations. One Na ion was placed on each of the top and bottom surfaces, but the two Mg ions were not allowed to occupy a neighboring octahedral site. This single-layer model is

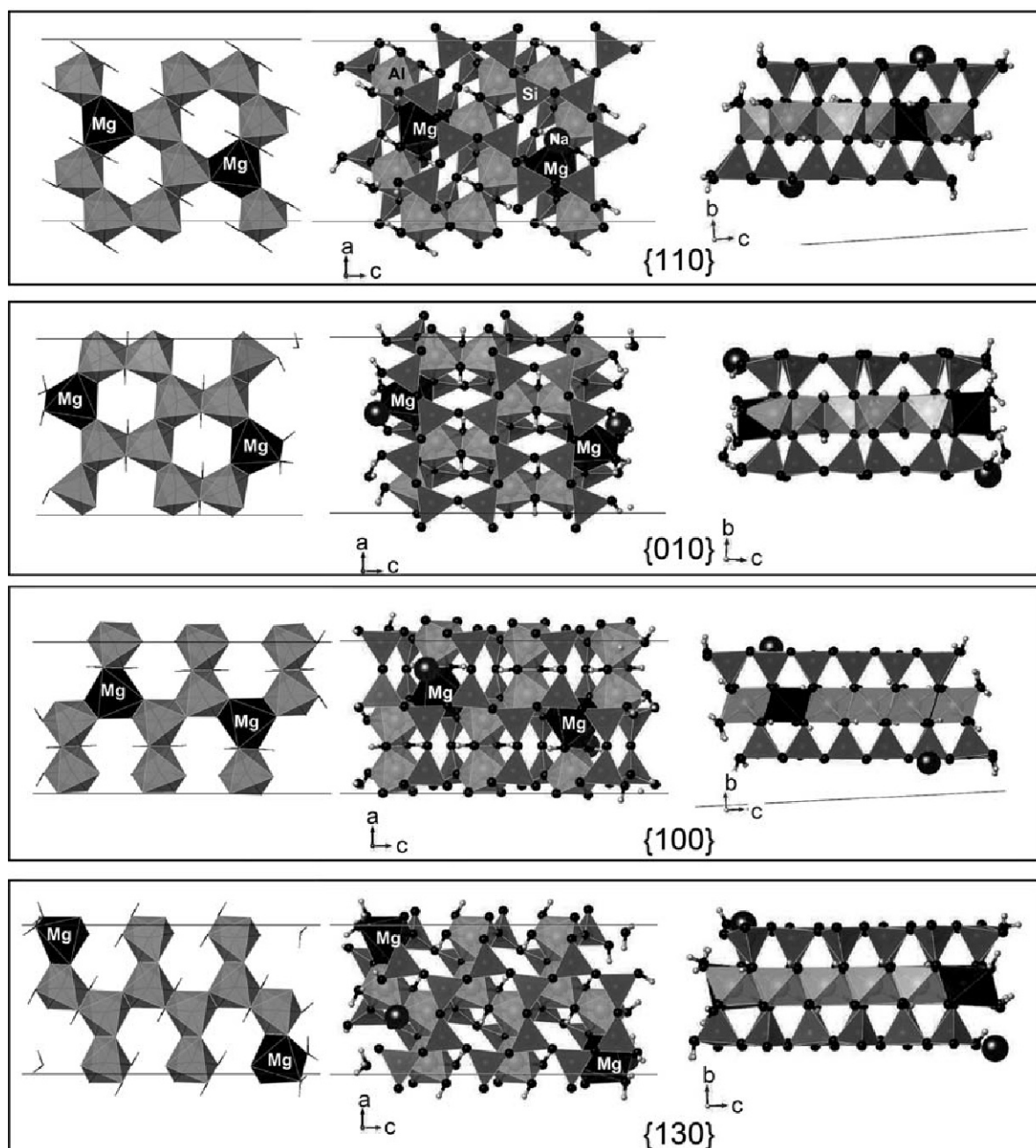


Figure 2. Top (center) and side (right) views of single-layer edge models for layer charge  $y = 0.33$ . The octahedral sheets are shown on the left to indicate the isomorphous substitutions. The edge faces are nearly parallel to the  $ab$  planes.

Table 1. Calculated and experimental montmorillonite unit cell constants and  $E_{\text{ILBE}}$  values.

	$y$	$a$ (Å)	$b$ (Å)	$c$ (Å)	$\beta$ (°)	$E_{\text{ILBE}}$ (meV/Å <sup>2</sup> )
Wyoming montmorillonite (Tsipursky and Drits, 1984)	0.26	5.18	8.98	10.10	99.5	
Panama montmorillonite (Tsipursky and Drits, 1984)	0.45	5.18	8.98	10.08	101.0	
DFT (PBE) (Voora <i>et al.</i> , 2011)	0.25	5.25	9.09	10.08	99.27	
This study (PBE)	0.33	5.24	9.09	10.01	101.5	−1.79
This study (PBE)	0.50	5.23	9.09	9.83	96.55	−3.37

sufficient to examine a dispersed montmorillonite monolayer in aqueous solutions; however, in order to understand the behavior of montmorillonite under low-humidity conditions, the effect of layer stacking in a 1M polytype was investigated for  $y = 0.50$  (this value was chosen to reduce computational costs by having a smaller number of atoms in the unit cell).

## COMPUTATIONAL DETAILS

### First-principles calculations

The total energy of montmorillonite with the edge faces, bulk montmorillonite, and an isolated H<sub>2</sub>O molecule were calculated using first-principles electronic state calculations based on DFT (Hohenberg and Kohn, 1964; Kohn and Sham, 1965). The generalized gradient approximation proposed by Perdew, Burke, and Ernzerhof (PBE) (Perdew *et al.*, 1996) was employed to determine the exchange-correlation energy. The valence electrons of atoms were explicitly treated using a pseudopotential method (Rappe *et al.*, 1990). The electronic wave functions were determined on the basis of the plane wave set with a cutoff energy of 60 Ry. The atomic position was relaxed to satisfy the convergence of total energy to <0.1 mRy and maximum force acting on all atoms to be <0.1 mRy/bohr. The reliability of the employed pseudopotentials was confirmed by comparing the lattice constants ( $a$ ,  $b$ ,  $c$ , and  $\beta$ ) of montmorillonite with experimental results (Tsipursky and Drits, 1984) (Table 1). These calculations were conducted for the  $1 \times 1 \times 2$  supercell with a  $4 \times 2 \times 1$  Monkhorst–Pack k-point mesh (Monkhorst and Pack, 1976). The calculated lattice constants were consistent with values calculated by

Voora *et al.* (2011) using the same method and with experimental values reported by Tsipursky and Drits (1984). No significant differences in the lattice constants were identified for differences in layer charge  $y$ .

The shape of the orthorhombic supercell used for the calculated edge faces of the single-layer montmorillonite (Table 2) was used to calculate the unit area of an edge face. The unit area of an edge face was calculated using the following equation:  $A$  (Å<sup>2</sup>) =  $a$  (Å)  $\times$   $10$  (Å) /  $\sin\theta$ , where the layer thickness was assumed to be 10 Å in the dry state without swelling and  $\theta$  is the angle between the edge face and the basal plane. Two edge faces were in the supercell and k-point sampling was only performed for the  $\Gamma$  point because of the large supercell used in the present study. The total energy difference between the sheet silicate minerals was determined using these computational methods (Sakuma, 2013; Sakuma and Suehara, 2015). All DFT calculations were conducted using Quantum-ESPRESSO computer software (Giannozzi *et al.*, 2009).

The surface energy of the edge faces can be affected by stacked layers because of interactions between adjacent layers in the stacked-layer model (Figure 3) and this effect should be evaluated by comparing the energies between the single and stacked layers.

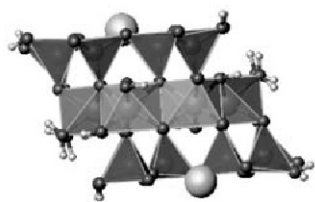
The surface energy  $E_{\text{surf}}$  of the single-layer model was calculated as follows:

$$E_{\text{surf}} = \frac{E_{\text{surf}}^{\text{mm}} - (E_{\text{bulk}}^{\text{mm}} + nE_{\text{gas}}^{\text{H}_2\text{O}} - 2A_{\text{basal}}E_{\text{ILBE}})}{2A} \quad (2)$$

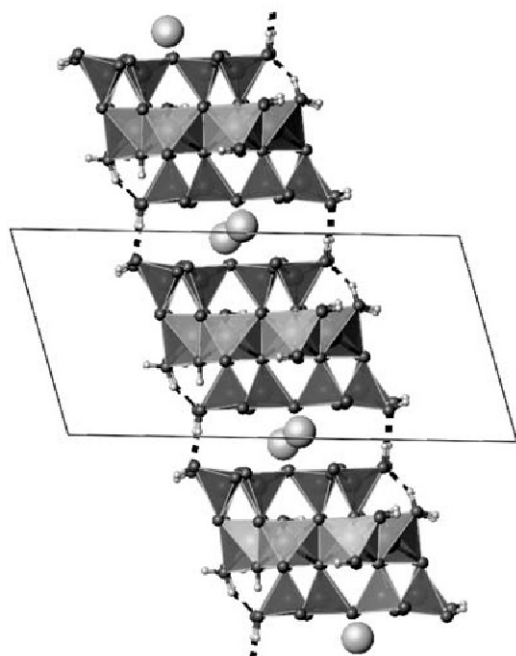
where  $E_{\text{surf}}^{\text{mm}}$  is the calculated total energy of the edge surfaces,  $E_{\text{bulk}}^{\text{mm}}$  is the energy of bulk montmorillonite,

Table 2. Shapes of the supercell used to calculate the surface energies of single-layer montmorillonite edge faces and the unit area of an edge face with two unit areas included in a supercell.

Edge faces	$a$ (Å)	$b$ (Å)	$c$ (Å)	$\sin\theta$	Unit area, $A$ (Å <sup>2</sup> )
{110}	10.513	36.751	50.000	0.98487	106.745
{010}	10.493	36.751	50.000	0.98487	106.542
{100}	9.0754	36.751	50.000	0.99487	91.222
{130}	9.0936	36.751	50.000	0.98001	92.791



### Single-layer model



### Stacked-layer model

Figure 3. The single-layer and stacked-layer models used to calculate the surface energy of edge faces. The solid line identifies the supercell used for the calculations. Periodic boundary conditions were applied normal to the page surface for both models. Hydrogen bonds between the SiOH groups of adjacent layers are shown by the dotted lines in the stacked-layer model.

$E_{\text{ILBE}}$  is the interlayer bonding energy of montmorillonite,  $E_{\text{H}_2\text{O}}^{\text{gas}}$  is the energy of an isolated  $\text{H}_2\text{O}$  molecule,  $n$  is the number of chemisorbed  $\text{H}_2\text{O}$  molecules on the edge faces,  $A_{\text{basal}}$  is the area of the basal plane, and  $A$  is the area of the edge face. The interlayer bonding energy is the energy that connects the basal planes of layered minerals together (Giese, Jr., 1973). The energy  $E_{\text{ILBE}}$  can be determined from the total energy difference between the relaxed structure of two bonded layers,  $E_{2\text{layer}}$ , and an isolated single layer,  $E_{1\text{layer}}$ , using the formula  $E_{\text{ILBE}} = E_{2\text{layer}} - 2E_{1\text{layer}}$  (Sakuma, 2015; Sakuma and Suehara, 2015). The surface energy per unit area was determined by summing the energy required to form edges with the hydration energy of  $\text{H}_2\text{O}$  molecules

chemisorbed to edge faces. Two edge faces were included in the supercell; therefore, the surface energy was the average energy of these two faces.

The surface energy of stacked-layer models was calculated using the following equation:

$$E_{\text{surf}} = \frac{E_{\text{surf}}^{\text{mm}} - (E_{\text{bulk}}^{\text{mm}} + nE_{\text{gas}}^{\text{H}_2\text{O}})}{2A} \quad (3)$$

with variables as defined in equation 2.

#### Variations in the locations of Na and Mg ions

The extent of isomorphic substitution of Mg for Al in octahedral sites varies, as illustrated by the various Mg sites in  $\{110\}$  edge faces for a layer charge of  $y = 0.50$  (Figure 4). Five configurations, denoted P1 to P5, for the isomorphic substitution of Mg for Al were considered for the initial configurations. To clarify the location and distance between Mg ions, the substituted locations were classified into three positions, such as outermost edge sites (E), near edge sites (N), and the other bulk sites (B). The notation “EEd6.1” indicates that two Mg ions occupy the outermost edge sites and the distance between the Mg ions is 6.1 Å. Plausible stable positions of interlayer Na ions are at the center of the ditrigonal ring of the montmorillonite surface. In these edge faces, the eight positions include four at the top and the bottom surfaces of each site, which were used as the initial Na ion configurations. In these 80 initial configurations, ionic optimization was conducted to obtain the surface energy of the edge faces.

The surface energy differences between the same isomorphic substitutions (Figure 5) were ascribed to the different positions of the Na ions. Most of the structures had positive surface energies, although negative surface energies were obtained for about 10% of the structural models tested. Such negative surface energies are unrealistic for a single-component system; however, a multicomponent system, such as a solid surface with chemisorbed and dissociated water molecules, can have a negative surface energy (Łodziana *et al.*, 2004; Mathur *et al.*, 2005; Newton and Sposito, 2015). The minimum energy in these isomorphic substitutions are discussed in the following sections. Similar procedures were conducted for four edges with two layer charges.

#### System-size effect on the surface energy of edge faces

The limited size of the system may affect the stability of isomorphic substitutions. Two systems in the unit cell were tested to compare the surface energy of edge faces with  $y = 0.5$ . One-unit and two-unit systems include 106 and 188 atoms in the unit cell, respectively (Figure 6). The difference between these systems is mainly the length of the bulk layer. The surface energy of the large system slightly changed from the small system due to the increased degree of freedom (Figure 6). The energy difference between small and large systems, however,

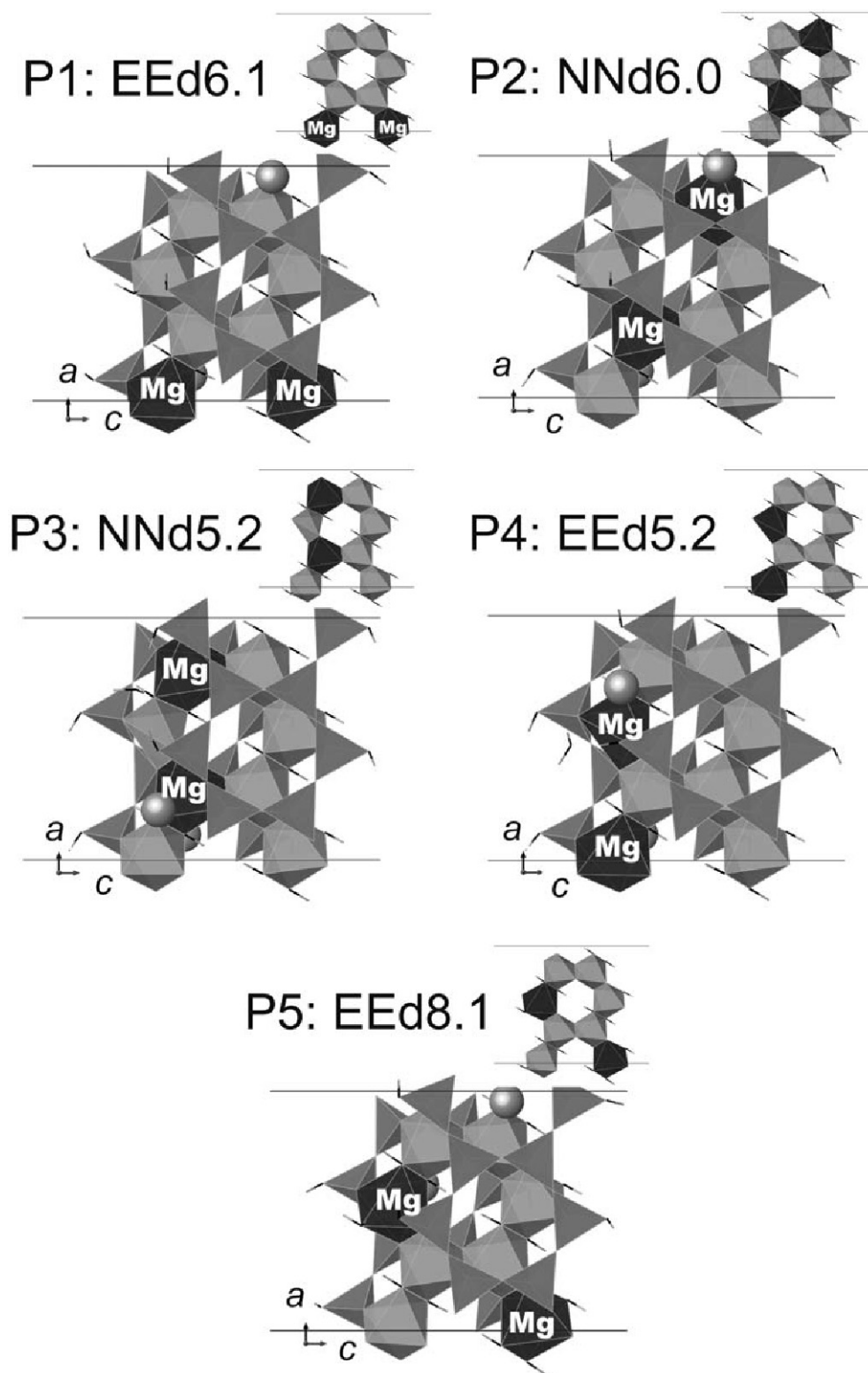


Figure 4. The five different isomorphous substitutions that were considered for the {110} edge faces of the single-layer model at  $y = 0.50$ . The notations, such as “EEd6.1”, indicate the location and distance between Mg ions as explained in the text. These are the most stable structures for the various locations of Mg and Na ions. The octahedral sheets are shown above to indicate the isomorphous substitutions.

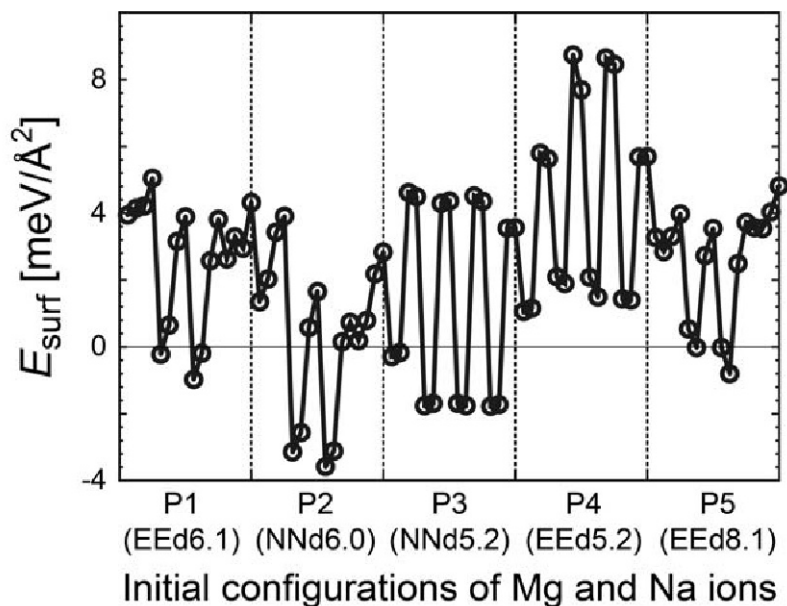


Figure 5. The surface energies of the  $\{110\}$  edge faces for the five different isomorphous Mg ion substitutions as shown in Figure 4 and the various locations of Na ions.

was  $<0.01$  eV/atom and was smaller than the typical energy of covalent ( $>1$  eV/bond), ionic ( $>1$  eV/bond), and hydrogen ( $>0.1$  eV/bond) bonds. The surface energies in order of decreasing energy were  $\{010\} > \{110\} > \{100\} > \{130\}$  and were estimated using the small system. This was identical to that calculated for the large system and, therefore, the conclusion was the same for both systems.

## RESULTS

### Interlayer bonding energy

The interlayer bonding energy ( $E_{ILBE}$ ) of montmorillonite was calculated using the same method that was previously reported for mica and clay minerals (Sakuma and Suehara, 2015). The interlayer bonding energies calculated in the present study were stronger for the high layer charge,  $y = 0.50$ , than for the low layer charge,  $y = 0.33$ . The  $E_{ILBE}$  values of the  $y = 0$  and  $y =$

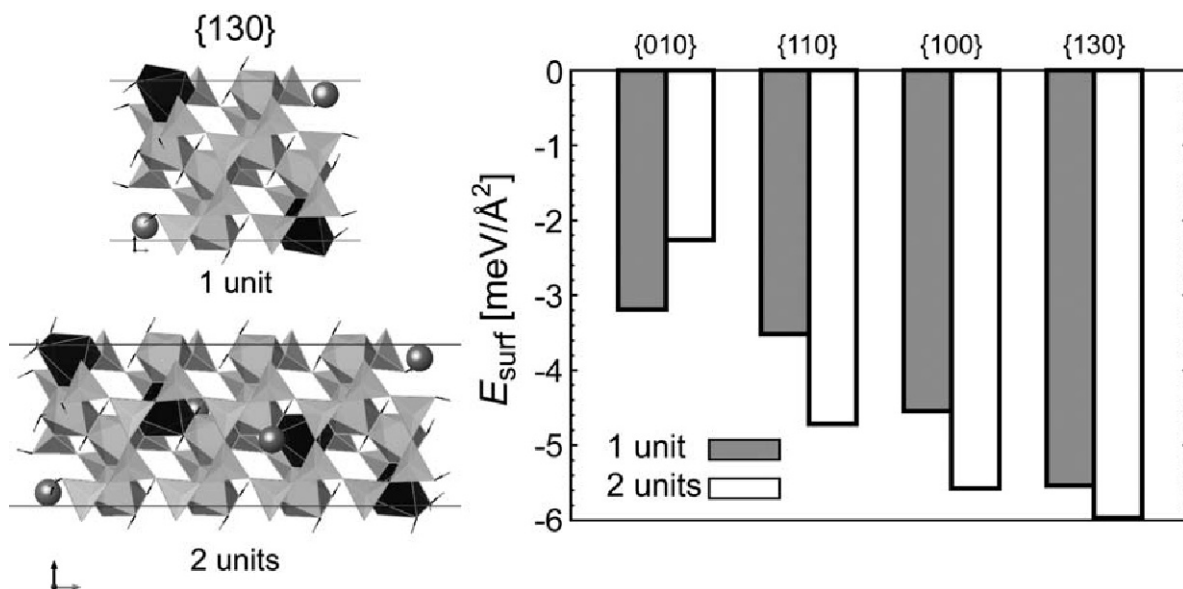


Figure 6. A comparison of the surface energies of edge faces calculated using one-unit and two-unit structures. The surface energies of the  $\{130\}$  edge faces of one-unit and two-unit structures are shown at left.



1.0 layer charges were derived from the results for pyrophyllite and muscovite (Sakuma and Suehara, 2015), respectively. The energy decreased with an increase in the layer charge (Figure 7). This change in the energy can be attributed to a strong Coulombic interaction between the layers of high layer charge minerals. It should explain the reason why the  $E_{ILBE}$  value of pyrophyllite was nearly zero. This would be unrealistic for considering stacked pyrophyllite layers in a natural environment. The PBE method usually underestimates the dispersion force; therefore, an empirical dispersion force correction has often been applied for pyrophyllite. The energy differences, however, between clay minerals determined using the PBE method are linearly related to the differences calculated using methods that included empirical corrections (Sakuma and Suehara, 2015). For the above reason, we discuss the energy differences between minerals using the pure PBE method.

#### Surface energy of edge faces for the layer charge of 0.50

*{110}* edge faces ( $y = 0.50$ ). The most stable configurations for the five models (P1 to P5) (Figure 4) have different surface energies (Figure 8). The energy differences imply that Mg is stable in the bulk part rather than near the edge faces and that the long interatomic distance between the two Mg ions is stable (Figure 4). The energy difference as a function of the average interatomic Na–Mg distance ( $d(\text{Na-Mg})$ ) and the interatomic Na–Na distance ( $d(\text{Na-Na})$ ) can be useful to understand the relationship between the structure and surface energy. These maps (Figure 9) indicate that Na ions are stable near Mg ions, which is reasonable because the isomorphous substitution of divalent Mg for trivalent Al ions creates a negative charge in the structure.

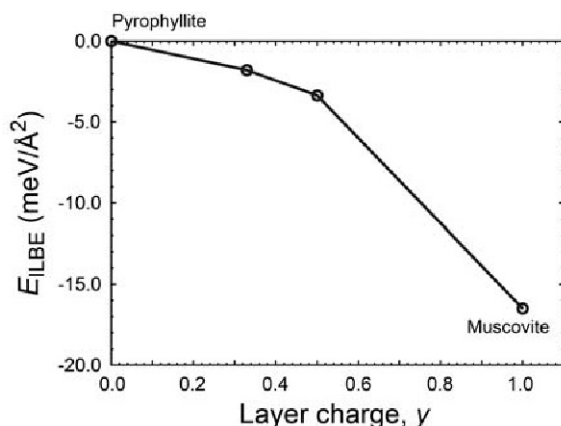


Figure 7. Interlayer bonding energies ( $E_{ILBE}$ ) calculated using the PBE method as a function of layer charge. The muscovite and pyrophyllite values were obtained from previous calculations (Sakuma and Suehara, 2015).

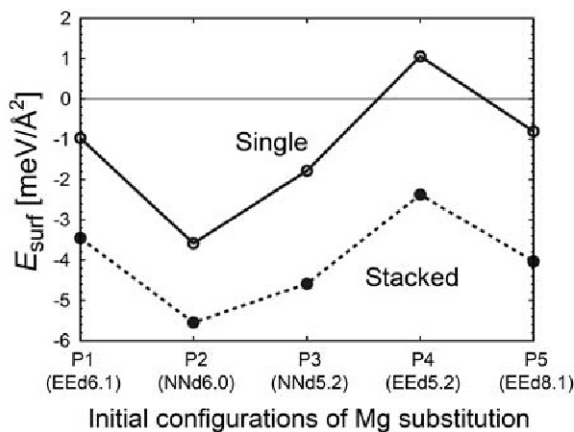


Figure 8. A comparison of the minimum surface energies for Mg substitutions in single and stacked layers.

The surface energy of the stacked-layer model was lower than that of the single-layer model (Figure 8). This can be attributed to SiOH group hydrogen bonds between adjacent layers, as shown by the dotted lines that connect the layers in the stacked-layer model (Figure 3). The four SiOH groups create hydrogen bonds between two layers.

*{010}* edge faces ( $y = 0.50$ ). The same analysis that was used for the *{110}* edge faces was conducted for the *{010}* edge faces for six different isomorphous substitutions of Mg for Al (Figure 10). The Na ions are stable near the Mg ions, which is indicated by the local negative charges near the  $\text{MgO}_6$  sites. The structure of P6 was the most stable for both the single and stacked models (Figure 10). A long interatomic distance between Mg ions is required to stabilize this edge face. The high surface energy that corresponds to unstable edge faces can be characterized by long Na–Mg distances and most low-energy areas are found at long Na–Na distances (see Supplementary Material section (deposited with the Editor-in-Chief and available at <https://www.clays.org/Journal/JournalDeposits.html>)).

No energy difference between the single-layer and stacked-layer models was observed for P3 and P6 (Figure 10), which was implied by the absence of hydrogen bonds between SiOH groups in the stacked model (Figure 10). The difficulty in creating the hydrogen bonds can be attributed to the structure of the *{010}* edge faces. The distance between SiOH groups in different layers at the *{010}* edge faces were longer than the distance for *{110}* edge faces. The energy of the stacked model was higher than that of the single-layer model for P1, P2, P4, and P5, which is completely different from that at the edge of *{110}*. A plausible explanation is that the Na and Mg distances can be smaller in the single-layer model than those in the stacked model. As demonstrated by the stable structure of P4 (Figure 10), the Na ions were stable near the edge faces in the single-layer model. In the stacked model,

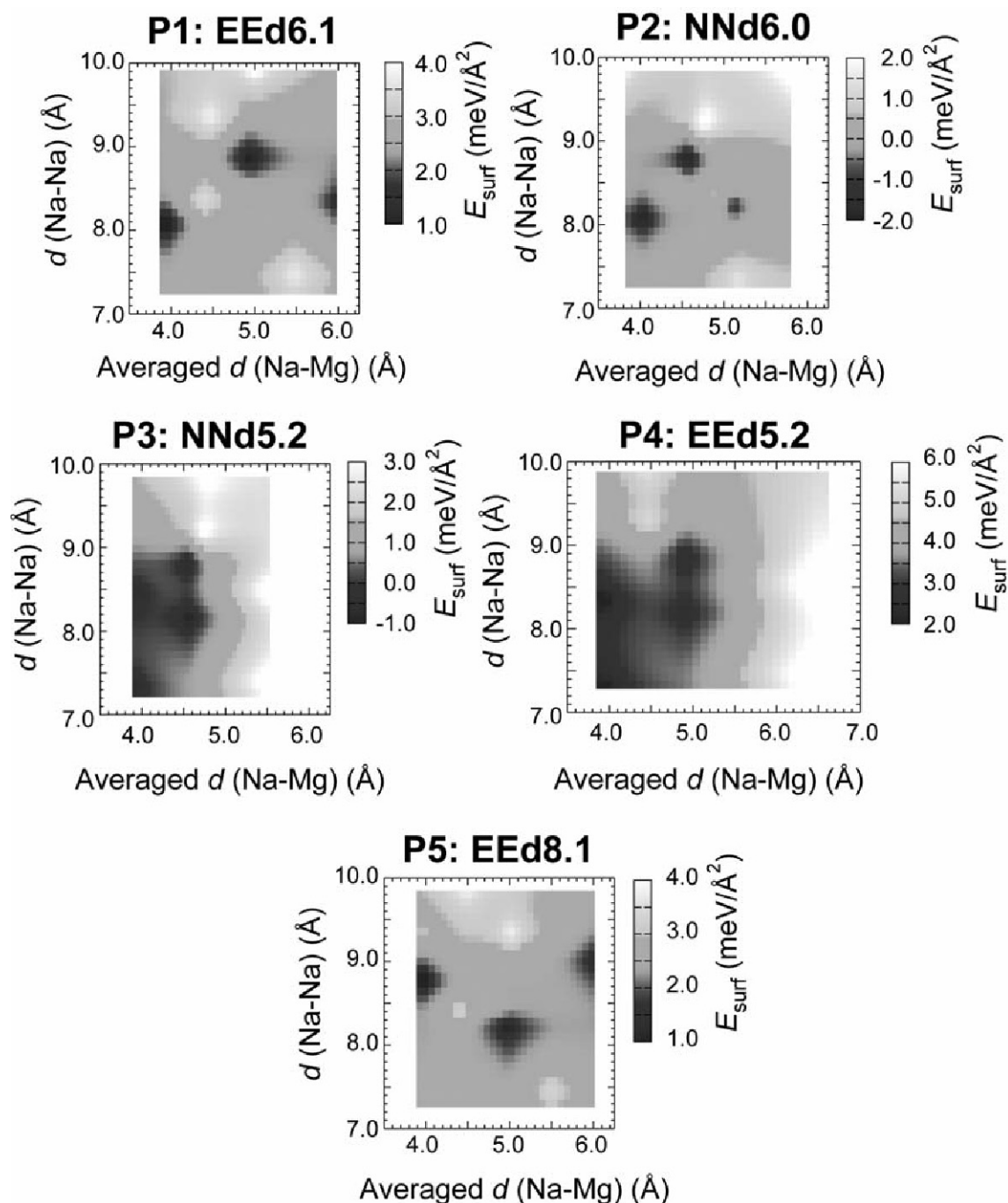


Figure 9. The surface energies of  $\{110\}$  edge faces for five different isomorphous Mg ion substitutions (P1 to P5) for a single montmorillonite layer as a function of average interatomic distance  $d(\text{Na-Mg})$  and  $d(\text{Na-Na})$ .

compensation of the negative charge of montmorillonite layers by only Na ions is impossible.

*$\{100\}$  edge faces ( $\gamma = 0.50$ ).* The Na ions were stable near octahedral Mg ions in a similar manner as those at the  $\{110\}$  and  $\{010\}$  edge faces (Figure 11). The most stable structure was P1, which indicates that the Mg should be in the bulk part of the structure to yield stable

edge faces. Low surface energy was obtained for short Na-Mg distances and long Na-Na distances (see Figure S2 in Supplementary Materials section (deposited with the Editor-in-Chief and available at <http://www.clay-s.org/JOURNAL/JournalDeposits.html>)). The decreased surface energy of the stacked model was indicated by hydrogen bonding networks at the edge faces as shown in the  $\{110\}$  edge faces.

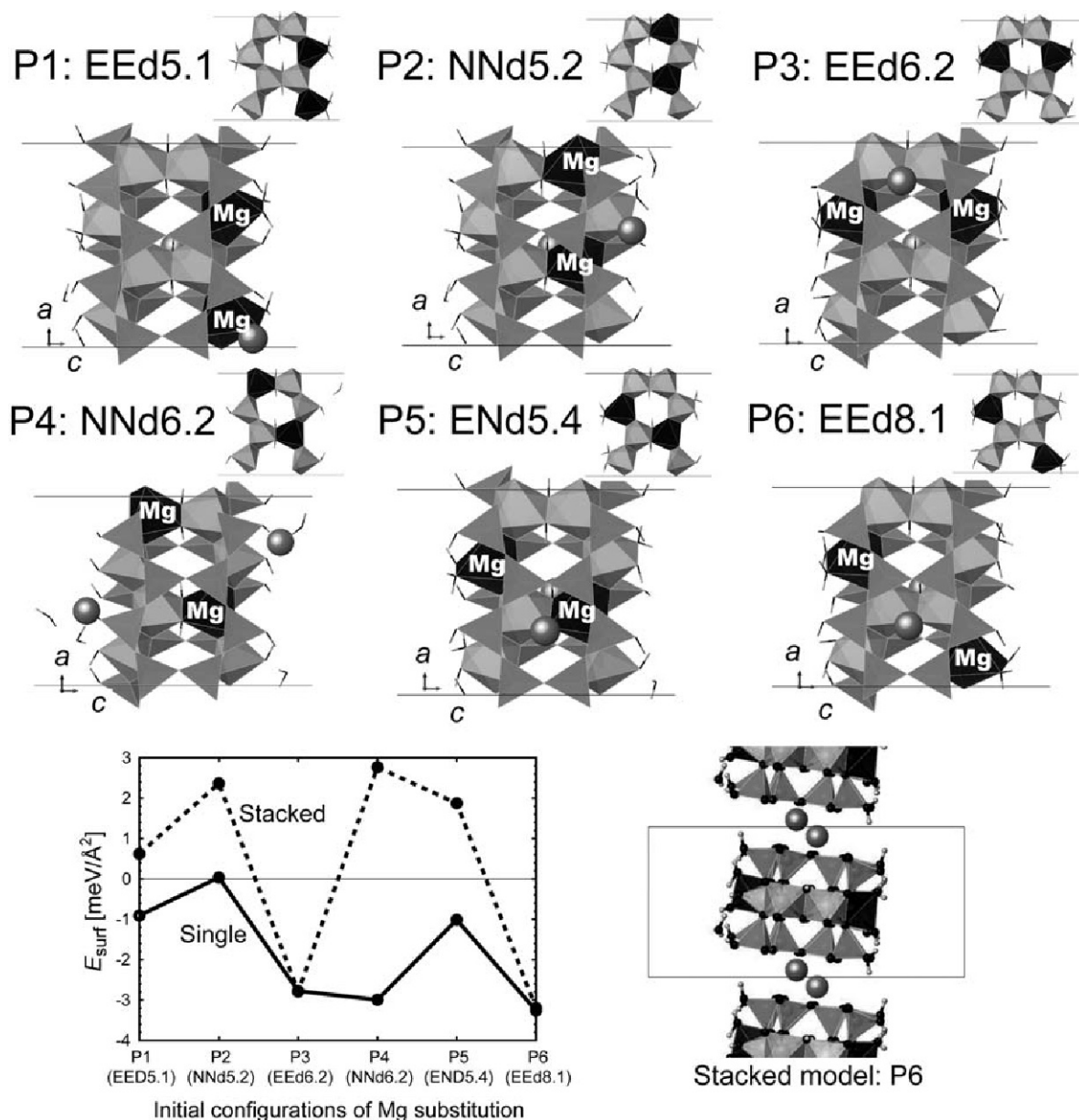


Figure 10. Six different isomorphous substitutions considered for the {010} edge faces for layer charge  $\gamma = 0.50$ . The octahedral sheets are shown at the top to indicate the isomorphous substitutions. The bottom left figure compares the minimum surface energies of these edge faces. The bottom right figure shows the stable structure of the P6 stacked-layer model. No clear hydrogen bonds were formed between the SiOH groups of adjacent layers.

*{130} edge faces ( $\gamma = 0.50$ ).* The Na ions were stable near octahedral Mg ions for all edge faces (Figure 12). The most stable structures were found for long Mg-Mg distances (P6). Low surface energy was obtained for short Na-Mg distances and long Na-Na distances (see Figure S3 in Supplementary Materials). Most configurations of the stacked model except for P2 decreased the surface energy relative to that in the single-layer model, which is explained by the hydrogen bonds between the layers of the stacked model.

#### *Surface energy of edge faces for a layer charge of 0.33*

Many combinations of isomorphous substitutions can be considered for the layer charge  $\gamma = 0.33$  as discussed for  $\gamma = 0.50$  in the previous sections. Here, symmetric edge faces were tested for  $\gamma = 0.33$  because such symmetric configurations were stable for all edges at  $\gamma = 0.50$ . The effect of stacking on the surface energy appears to depend on the presence of hydrogen bonds between the SiOH groups rather than isomorphous substitutions and, therefore, the single-layer model was used here.

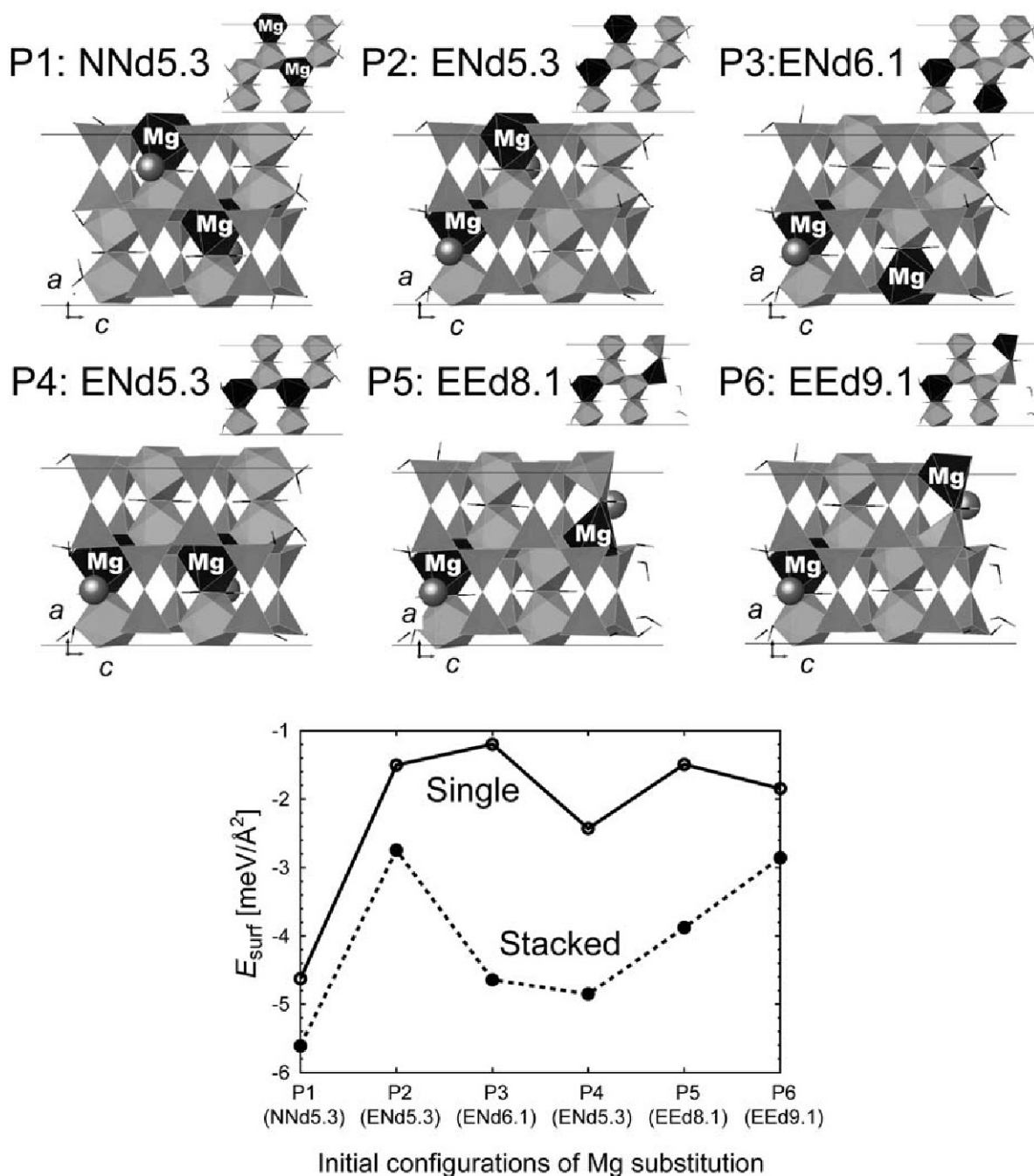


Figure 11. Six different isomorphous substitutions considered for the  $\{100\}$  edge faces for layer charge  $\gamma = 0.50$ . The octahedral sheets are shown at the top to indicate the locations of the isomorphous substitutions. The bottom figure compares the minimum surface energies of these edge faces for various initial Mg positions.

$\{110\}$  edge faces ( $\gamma = 0.33$ ). Two Mg ions were included in the isomorphous substitutions of these structures (Figure 13). The surface energy differences between the three different isomorphous substitutions indicate that P2 was more stable than P1 and P3. The energy difference implies that the Mg is stable in the bulk part of the structure rather than at the edge. When the

Mg-Mg distance was long, such as that shown in the P1 and P2 structures, the stable structures were characterized by long Na-Na and short Na-Mg distances (see Figure S4 in Supplementary Materials). If the Mg-Mg distance is short, such as that in the P3 structure, the Na-Na distance can also be short due to the strong attractive interactions between the Na and Mg ions.

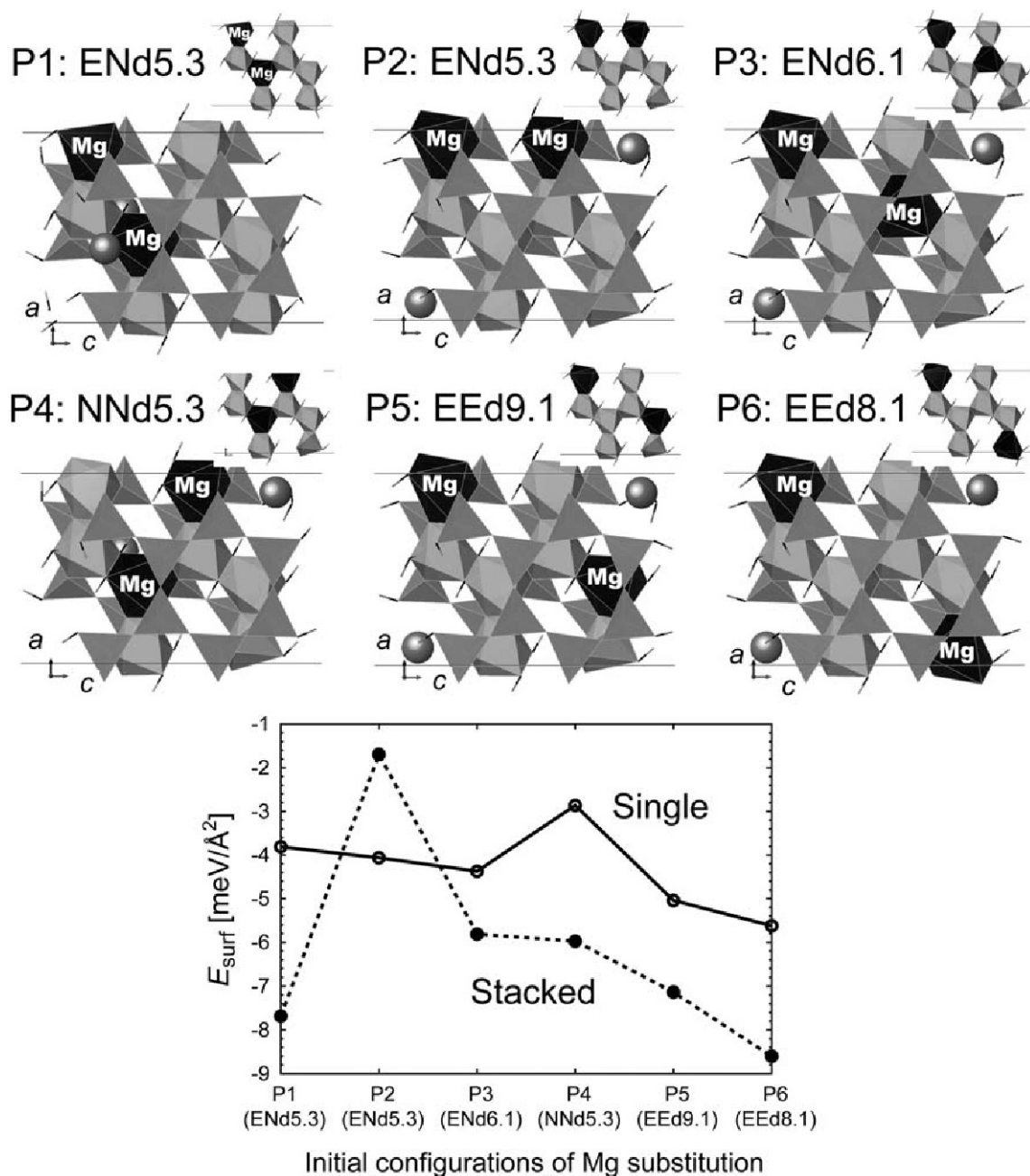


Figure 12. Six different isomorphous substitutions considered for the {130} edge faces for layer charge  $\gamma = 0.50$ . The octahedral sheets are shown at the top to indicate the isomorphous substitutions. The bottom figure compares the minimum surface energies of these edge faces for various initial Mg positions.

*{010} edge faces ( $\gamma = 0.33$ ).* The Na ions were stable near Mg ions (Figure 14). The most stable structure was P1, which can be attributed to the strong attractive interactions between Mg and Na ions at the edge faces. The relationship between the surface energy and interatomic distances was similar to those for the {110} faces with stable short Na-Mg and long Na-Na distances (see Figure S5 in Supplementary Materials).

This was not the case for P3 because the short Mg-Mg distance created a stable local structure at the short Na-Na site distance due to the strong attractive interactions between the Mg and Na ions.

*{100} edge faces ( $\gamma = 0.33$ ).* In the stable structures of four different isomorphous substitutions (Figure 15), the P2 and P3 models were more stable than P1, which

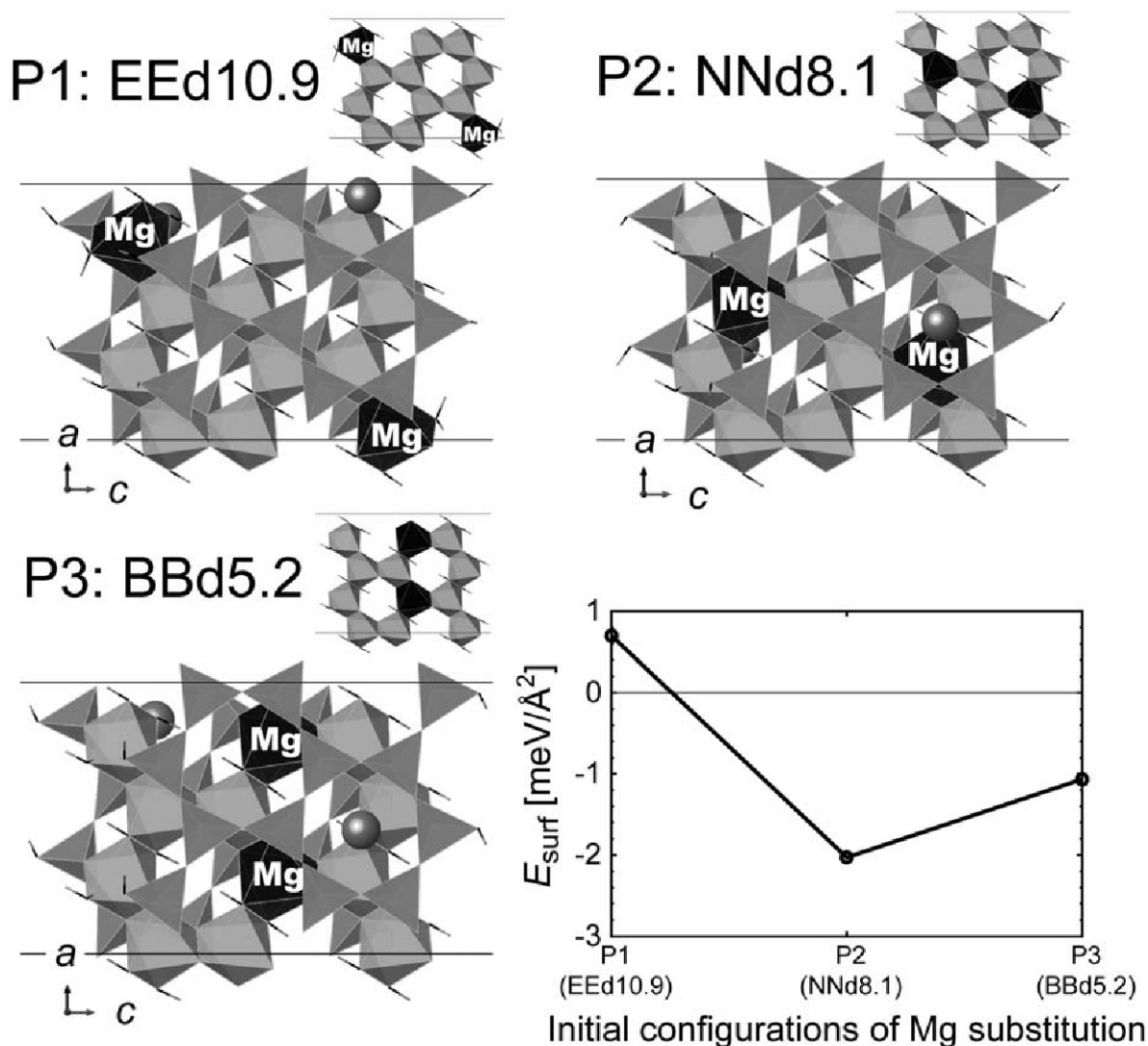


Figure 13. Three different isomorphous substitutions considered for the {110} edge faces for layer charge  $\gamma = 0.33$ . The octahedral sheets are shown at the top to indicate the isomorphous substitutions. The bottom right figure compares the minimum surface energies of these edge faces for various initial Mg positions.

indicates that the Mg ions are stable in the bulk part of the structure rather than near the edge faces. A small energy difference between the P2 and P4 models was implied by the high repulsive energy created by the short Mg-Mg distance in the P4 model. The relationship between the surface energy and Na-Na and Na-Mg distances (see Figure S6 in Supplementary Materials) is similar to that of the {110} and {010} edge faces.

*{130} edge faces ( $\gamma = 0.33$ ).* The energy difference between four different isomorphous substitutions indicates that the short Mg-Mg distance is unstable in these structures (Figure 16). The relationship between the surface energy and the Na-Na and Na-Mg distances (see Figure S7 in Supplementary Materials) is similar to that in the other edge faces tested in the present study.

## DISCUSSION

### *Difference between stacked- and single-layer models*

The surface energy of the stacked model was lower than that of the single-layer model for the {110}, {100}, and {130} edge faces, which is implied by the presence of hydrogen bonds between the SiOH groups of adjacent layers. The hydrogen-bonding energy was estimated to be 2–3  $\text{meV}/\text{\AA}^2$  in our model. This value was based on the assumption that the energy of hydrogen bonds between the SiOH and  $\text{SiO}_4$  groups was 2.7 to 4.1 kcal/mol, which was based on the energy of  $\text{Si}(\text{OH})_4$  adsorption to a kaolinite surface with terminal  $\text{SiO}_4$  groups (Han *et al.*, 2016). This is consistent with the energy difference between the single and stacked layers of the {110} edge faces. This difference in surface energy indicates that the stacking of clay minerals can

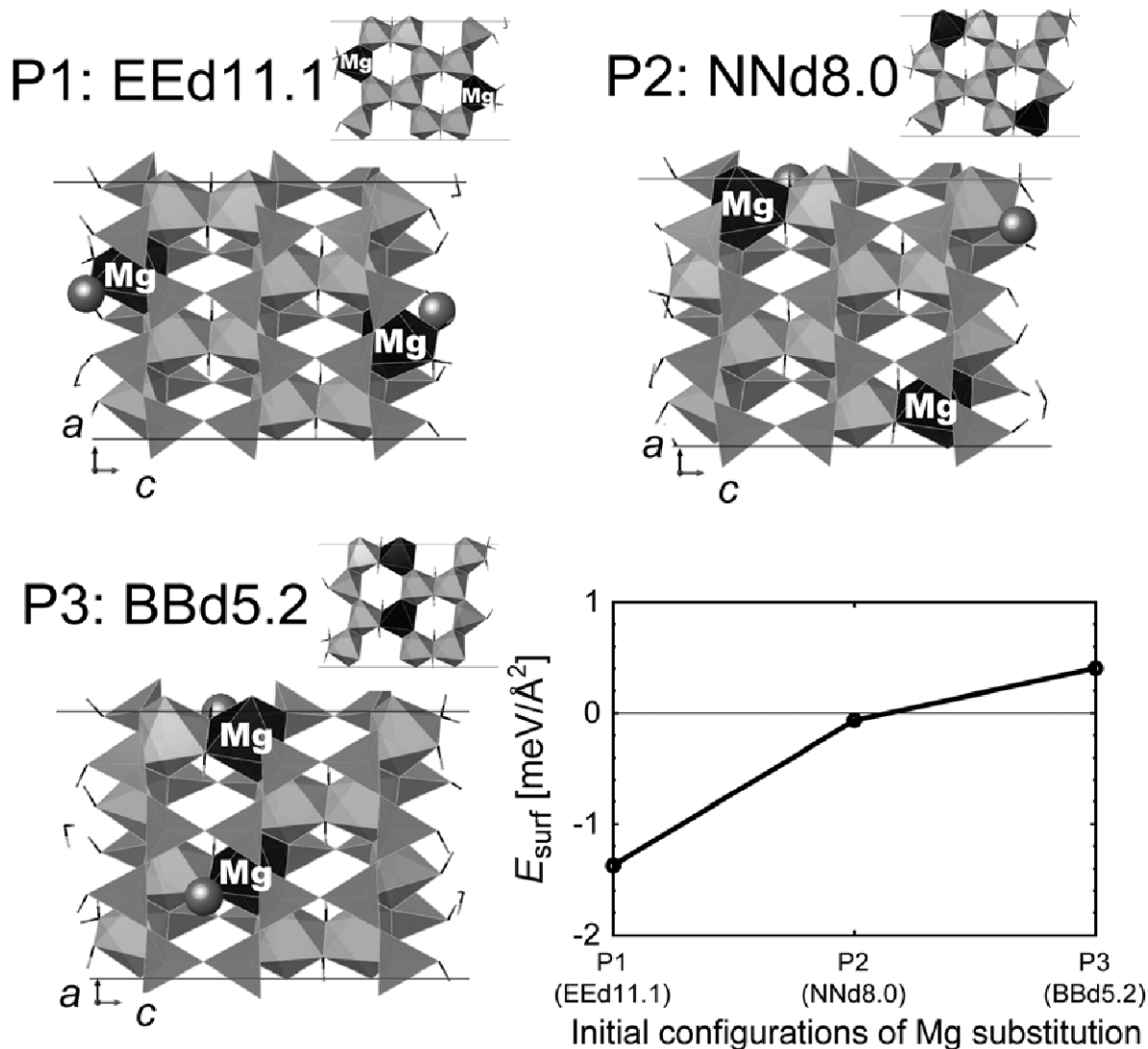


Figure 14. Three different isomorphous substitutions considered for the {010} edge faces for layer charge  $y = 0.33$ . The octahedral sheets are shown at the top to indicate the isomorphous substitutions. The bottom right figure compares the minimum surface energies of these edge faces for various initial Mg positions.

stabilize the edge faces. A 1M polytype was assumed for these stacked models. Different polytypes create different stacking structures and the hydrogen bonds at the edges differ from that in a 1M polytype.

#### Stability of Mg ions and positive ion adsorption sites on the edge faces

The stable Mg substitutions (Table 3) were clearly correlated with the edge face type. No confirmed correlation was observed between stable Mg substitutions and layer charge in all of the edges tested in this study. The stability of the Mg substitutions in the {110} edge faces were consistent with previous DFT research that used different layer charges (Newton *et al.*, 2016). The differences between the stable Mg substitutions in the

edge faces can be attributed to the number of shared O atoms between the MgO<sub>6</sub> octahedra, AlO<sub>6</sub> octahedra, and

Table 3. Stable Mg positions in the edge models where the term “edge” indicates the MgO<sub>6</sub> octahedra located at the outermost positions of edge faces. The term “bulk” distinguishes the MgO<sub>6</sub> octahedra in the bulk structure from the “edge” positions.

Edge faces	$y = 0.5$	$y = 0.33$
{110}	bulk	bulk
{010}	edge	edge
{100}	bulk	bulk
{130}	edge	edge

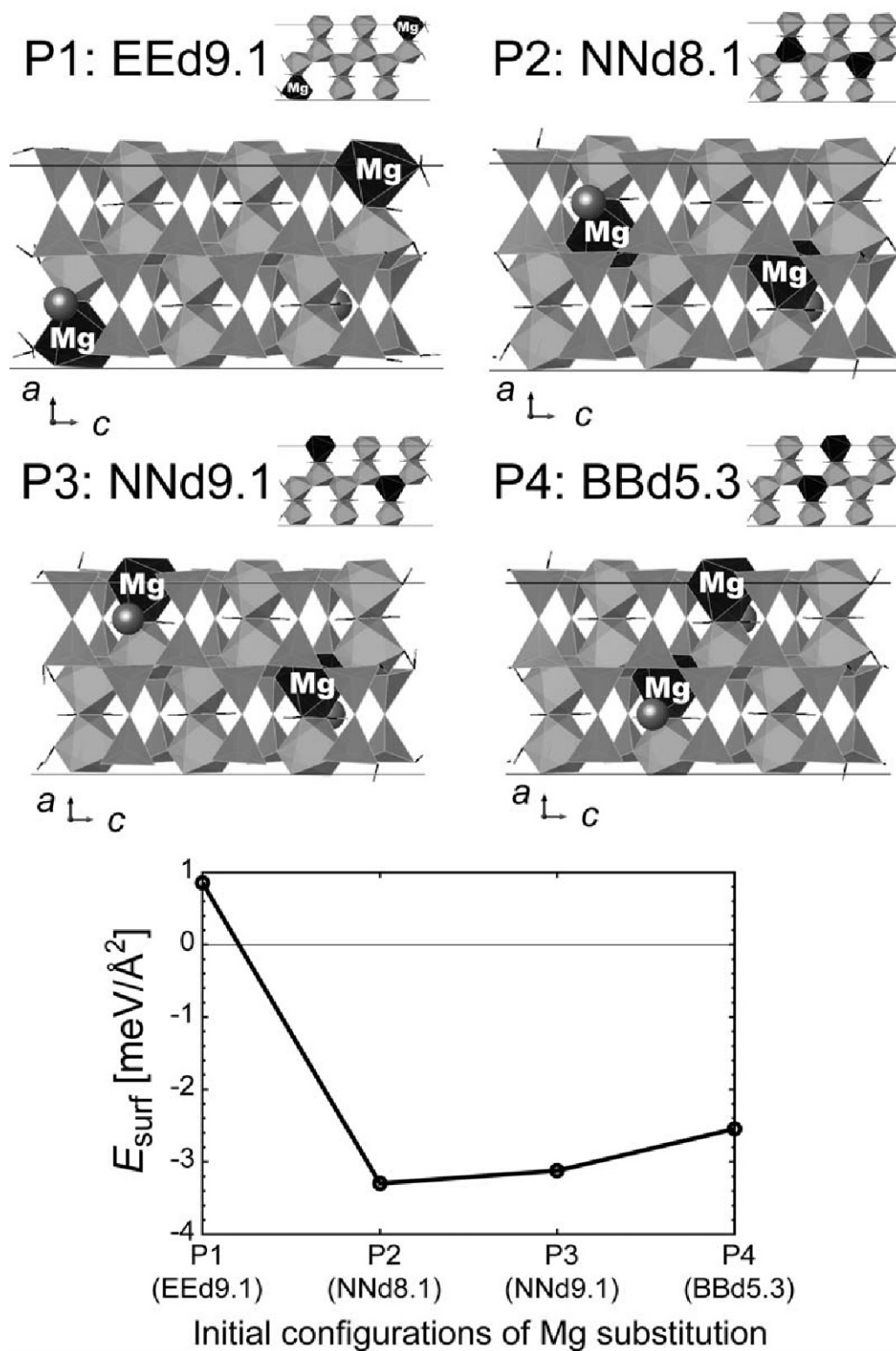


Figure 15. Four different isomorphous substitutions considered for the  $\{100\}$  edge faces for layer charge  $\gamma = 0.33$ . The octahedral sheets are shown at the top to indicate the isomorphous substitutions. The bottom figure compares the minimum surface energies of these edge faces for various initial Mg positions.



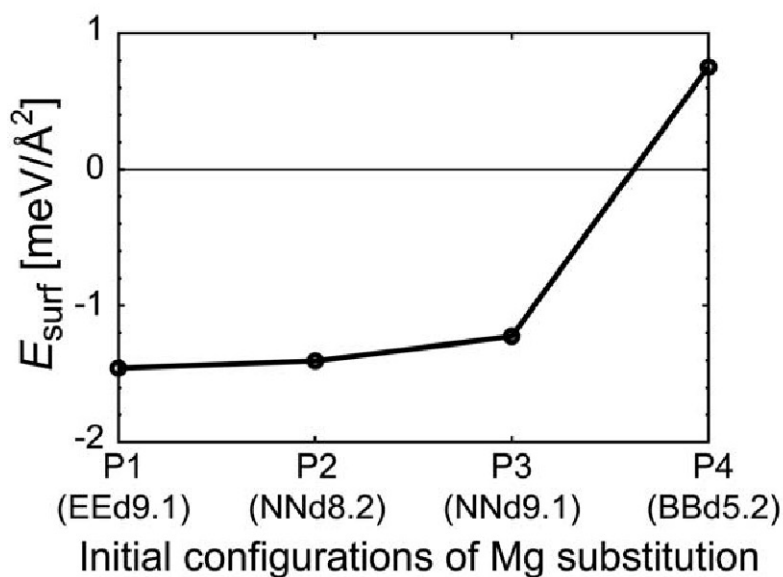
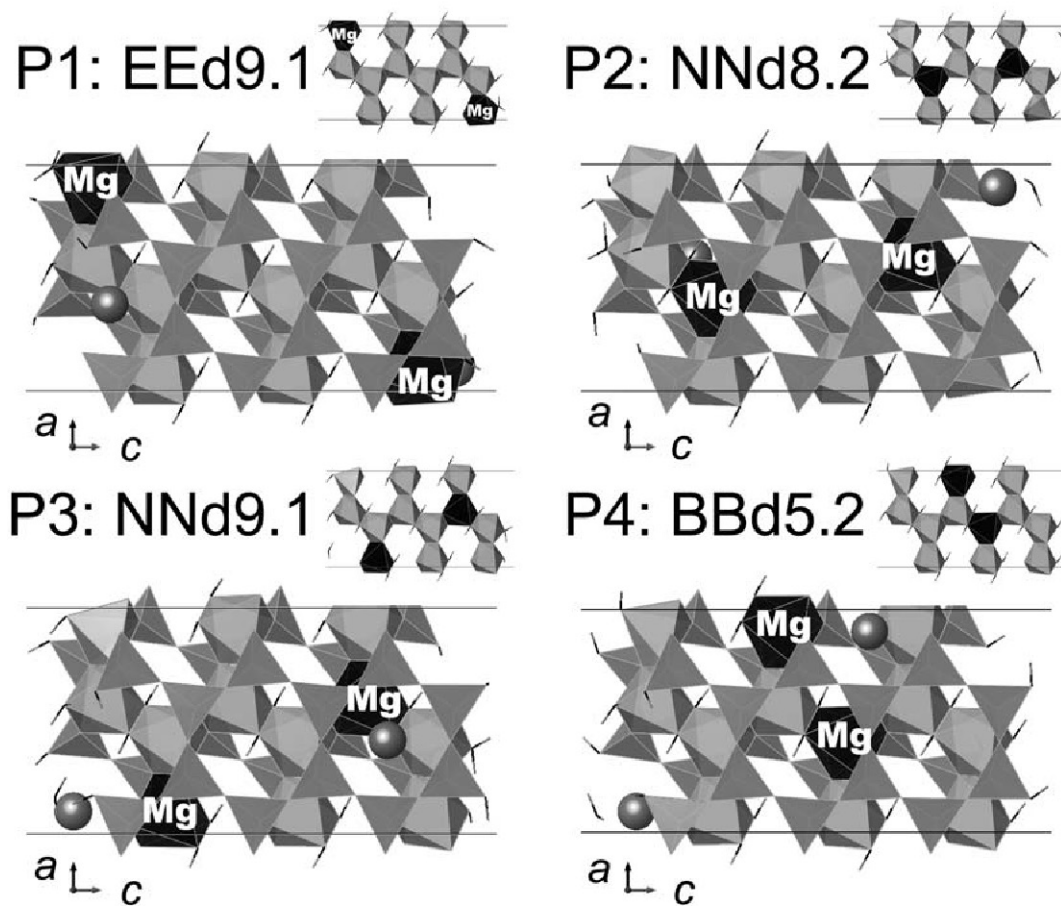


Figure 16. Four different isomorphic substitutions considered for the {130} edge faces for layer charge  $\gamma = 0.33$ . The octahedral sheets are shown at the top to indicate the isomorphic substitutions. The bottom figure compares the minimum surface energies of these edge faces for various initial Mg positions.

SiO<sub>4</sub> tetrahedra. In the bulk structure, all O atoms are shared by at least two polyhedra, but unshared O atoms can be present at edge faces. Although the charge of unshared O atoms is partially compensated by chemisorbed hydrogen atoms, the partial negative charge can be larger than that of shared O atoms. This large negative charge can stabilize the Mg substitutions. The MgO<sub>6</sub> octahedra of the {010} and {130} edge faces have two

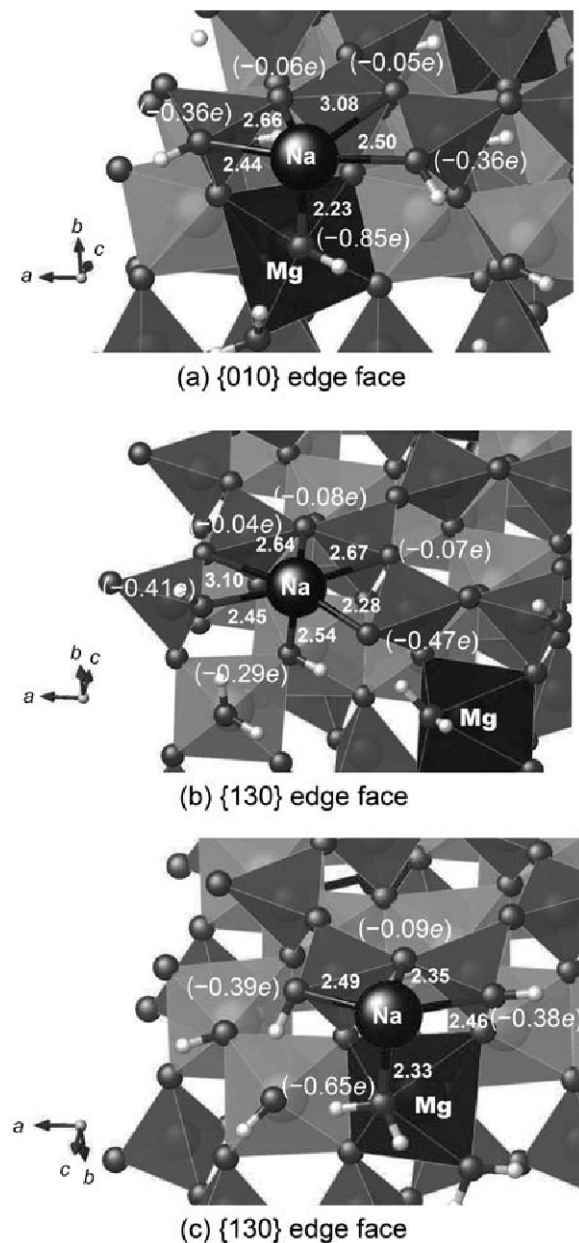


Figure 17. Structure (a) of adsorbed Na ions at {010} and {130} edge faces. Two stable Na adsorption sites were obtained for the {130} faces as shown in (b) and (c). The numbers indicate the distance (Å) between the adsorbed Na ion and the surrounding O atoms. The numbers in parentheses indicate the calculated Löwdin charges of the surrounding O atoms.

unshared O atoms, whereas the octahedra of {110} and {100} edge faces have only one unshared O atom. The presence of two unshared O atoms at the {010} and {130} edge faces can result in stabilized Mg ions in comparison with the {110} and {100} edge faces. The interlayer Na ions were stable near the substituted Mg sites as shown by the relationship between the Na-Mg distance and the surface energy. These results imply that positively charged ions strongly adsorb to the {010} and {130} edge faces rather than to the {110} and {100} edge faces. The coordination number of O atoms around the Na ion at the {010} edge face was 5 and coordination numbers of the {130} faces were 6 and 4 according to the number of O atoms within the cutoff distance of 3.1 Å (Figure 17). The presence of the surrounding water molecules increases the coordination number through hydration. This result provides a plausible structural model to analyze clay mineral adsorption sites by comparison to the Extended X-ray Absorption Fine Structure results (EXAFS) (Bostick *et al.*, 2002; Fan *et al.*, 2014) and NMR methods (Tansho *et al.*, 2016). To confirm the charge distribution between atoms, the partial charges of atoms were calculated using Löwdin population analysis implemented in Quantum-ESPRESSO computer software (Giannozzi *et al.*, 2009). The largest partial charges of  $-0.85e$  and  $-0.65e$  were obtained for O atoms in MgO<sub>6</sub> octahedra at these edge faces (Figure 17). The charges that ranged from  $-0.29e$  to  $-0.47e$  for O atoms in SiO<sub>4</sub> tetrahedra and AlO<sub>6</sub> octahedra were larger than those that ranged from  $-0.04e$  to  $-0.09e$  for O atoms in the bulk structure. This result indicates that these edge sites have a local negative charge, which is enhanced by the presence of a MgO<sub>6</sub> octahedron at these edge faces and, therefore, it strongly adsorbs cations.

*Comparison of the surface energies for layer charges of  $y = 0.50$  and  $y = 0.33$*

The lowest surface energies were at  $y = 0.50$  and were lower than those at  $y = 0.33$  for all edge faces (Figure 18), which indicates that the edge faces at  $y = 0.50$  are more stable than those at  $y = 0.33$  in the

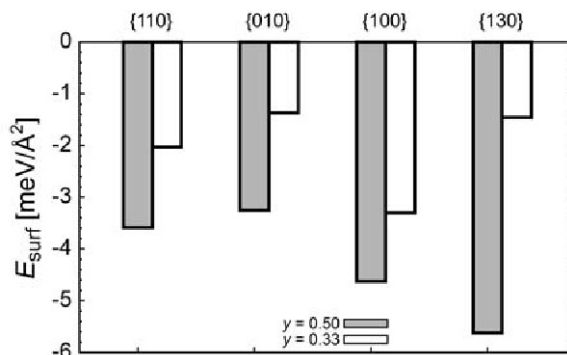


Figure 18. Lowest surface energies of the four edge faces for layer charges of  $y = 0.50$  and  $0.33$ .

presence of water. The size and morphology of clay minerals is important in estimating ion adsorption sites. The difference between edge face types with the same layer charge was small; therefore, identifying the dominant edge face in montmorillonite was difficult. Negative surface energy values were achieved due to the presence of chemisorbed water molecules on the edge faces. These edge faces were highly reactive and were stabilized in the presence of water. Once the surfaces are hydroxylated, crystal growth can be difficult due to the high energy barrier to remove chemisorbed water molecules from the edge faces. This effect was stronger for the high  $y = 0.50$  layer charge than for  $y = 0.33$ . The mechanism of crystal growth, however, is not simple for clay minerals which have many defects (Meunier, 2006) and, therefore, further research is needed to understand the crystal growth of clay minerals.

#### *Solvation effect on the edge faces*

In the present study, the structure and stability of edge faces with a few water molecules chemically adsorbed in a vacuum were considered, but the structure and stability can be changed by the presence of liquid water near the surface. A comparison between edge faces in a vacuum and edge faces in contact with a solution was conducted for pyrophyllite using the first-principles method (Churakov, 2007). The edge geometries are qualitatively similar, but the lengths of chemical bonds are slightly affected by the presence of water. The stiffer Si-O bonds were hardly changed by the presence of water, but the length of the relatively soft Al-O bonds was changed by the presence of hydrogen bonds. The strength of Mg-O bonds can be weaker than that of Al-O bonds based on the bond valence model (Brown, 2002); the Mg-O bond length at {010} and {130} edges, which have stable Mg substitutions at the edges, can, therefore, be altered by the presence of water.

Protonation and deprotonation are critical for cation adsorption to edge faces in the presence of water (Kremleva and Krüger, 2016). The Mg-OH<sub>2</sub>OH<sub>2</sub> acidity constant for the {010} edge face at  $y = 0.25$  was estimated to be 13.2 using a first-principles calculation and indicated that the protonated state supports common pH values (Liu *et al.*, 2013). This discussion may be applicable to the present system, but the actual acidity constants should be estimated for  $y = 0.33$  and 0.50 for further discussion. The acidity constants of Si-OH and Al-OH<sub>2</sub> groups were estimated to be smaller than 10 (Liu *et al.*, 2013) and the protonation state should be carefully considered depending on the solution pH.

#### CONCLUSIONS

The structure and stability of the four montmorillonite {110}, {010}, {100}, and {130} edge faces were examined using density functional theory. The surface energy of the edge faces for layer charges of  $y = 0.50$  and

$y = 0.33$  ( $e^-/\text{Si}_4\text{O}_{10}$ ) had negative values in the presence of chemisorbed water molecules. The surface energy was lower at the high layer charge (0.50) relative to the surface energy at the low layer charge (0.33), which implies that the size and morphology of a single crystal of montmorillonite can be altered by changes in the layer charge.

To examine the effect of stacking on the stability of the edge faces, the surface energies of stacked layers and single layers were examined. The surface energies of the edge faces for most of the stacked layers were reduced relative to the single-layer models due to the presence of hydrogen bonds between the layers at the edge faces. This indicates that the stability of the edge faces can be altered by the degree of swelling. Such a stacked-layer model is necessary to simulate non-swelling clays and mica minerals because the surface energy calculated with a single-layer model would otherwise overestimate the surface energy. In the present study, a stacked-layer model was constructed on the basis of a 1M polytype structure. The stacking structure was shown to depend on the polytype, but further discussion is required to apply the results to various clay minerals.

The location of Mg for Al isomorphous substitutions in octahedra is related to the location of interlayer cations. Stable Na ions on the ditrigonal rings in the interlayer space were examined to identify the ring nearest to the Mg ion location. The lowest surface energies of the {010} and {130} edge faces occurred for Mg ions located on the edge faces. These edge faces provide strong cation adsorption sites due to the local negative charge of the edges, which implies that montmorillonite morphology is related to the number of strong cation adsorption sites. These results contribute to an understanding of the structure, stability, and cation adsorption sites of montmorillonite edge faces. Various divalent and trivalent cations can substitute for the cations in the octahedral and tetrahedral sites of clay minerals. In future research, the effects of different elements on isomorphous substitutions at the edge faces should be investigated to determine the fundamental physics and chemistry of clay minerals.

#### ACKNOWLEDGMENTS

This research was partially performed as a part of “The project for validating assessment methodology in geological disposal system” and “The project for developing advanced geological repository concept and performance assessment methodology” funded by the Ministry of Economy, Trade, and Industry of Japan. The calculations in this study were partially performed using the Numerical Materials Simulator at NIMS. Comments by the associate editor and two anonymous reviewers greatly improved this manuscript.

#### REFERENCES

- Bickmore, B.R., Rosso, K.M., Nagy, K.L., Cygan, R.T., and Tadanier, C.J. (2003) *Ab initio* determination of edge surface structures for dioctahedral 2:1 phyllosilicates:

- Implications for acid-base reactivity. *Clays and Clay Minerals*, **51**, 359–371.
- Bleam, W.F., Welhouse, G.J., and Janowiak, M.A. (1993) The surface Coulomb energy and proton Coulomb potentials of pyrophyllite {010}, {110}, {100}, and {130} edges. *Clays and Clay Minerals*, **41**, 305–316.
- Bostick, B.C., Vairavamurthy, M.A., Karthikeyan, K.G., and Chorover, J. (2002) Cesium adsorption on clay minerals: An EXAFS spectroscopic investigation. *Environmental Science & Technology*, **36**, 2670–2676.
- Bowers, G.M., Bish, D.L., and Kirkpatrick, R.J. (2008) H<sub>2</sub>O and cation structure and dynamics in expandable clays: <sup>2</sup>H and <sup>39</sup>K NMR investigations of hectorite. *Journal of Physical Chemistry C*, **112**, 6430–6438.
- Brown, I.D. (2002) *The Chemical Bond in Inorganic Chemistry: The Bond Valence Model*. Oxford University Press, Oxford, 289 pp.
- Cheng, L., Fenter, P., Nagy, K.L., Schlegel, M.L., and Sturchio, N.C. (2001) Molecular-scale density oscillations in water adjacent to a mica surface. *Physical Review Letters*, **87**, 156103.
- Churakov, S.V. (2006) *Ab initio* study of sorption on pyrophyllite: Structure and acidity of the edge sites. *Journal of Physical Chemistry B*, **110**, 4135–4146.
- Churakov, S.V. (2007) Structure and dynamics of the water films confined between edges of pyrophyllite: A first principle study. *Geochimica et Cosmochimica Acta*, **71**, 1130–1144.
- Fan, Q.H., Tanaka, M., Tanaka, K., Sakaguchi, A., and Takahashi, Y. (2014) An EXAFS study on the effects of natural organic matter and the expandability of clay minerals on cesium adsorption and mobility. *Geochimica et Cosmochimica Acta*, **135**, 49–65.
- Ferrage, E., Lanson, B., Sakharov, B.A., and Drits, V.A. (2005) Investigation of smectite hydration properties by modeling experimental X-ray diffraction patterns: Part I: Montmorillonite hydration properties. *American Mineralogist*, **90**, 1358–1374.
- Ferrage, E., Lanson, B., Michot, L.J., and Robert, J.L. (2010) Hydration properties and interlayer organization of water and ions in synthetic Na-smectite with tetrahedral layer charge. Part I. Results from X-ray diffraction profile modeling. *Journal of Physical Chemistry C*, **114**, 4515–4526.
- Giannozzi, P., Baroni, S., Bonini, N., Calandra, M., Car, R., Cavazzoni, C., Ceresoli, D., Chiarotti, G.L., Cococcioni, M., Dabo, I., Dal Corso, A., de Gironcoli, S., Fabris, S., Fratesi, G., Gebauer, R., Gerstmann, U., Gougoussis, C., Kokalj, A., Lazzeri, M., Martin-Samos, L., Marzari, N., Mauri, F., Mazzarello, R., Paolini, S., Pasquarello, A., Paulatto, L., Sbraccia, C., Scandolo, S., Sclauzero, G., Seitsonen, A.P., Smogunov, A., Umari, P., and Wentzcovitch, R.M. (2009) QUANTUM ESPRESSO: A modular and open-source software project for quantum simulations of materials. *Journal of Physics: Condensed Matter*, **21**, 395502.
- Giese, Jr., R. F. (1973) Interlayer bonding in kaolinite, dickite and nacrite. *Clays and Clay Minerals*, **21**, 145–149.
- Han, Y., Liu, W., and Chen, J. (2016) DFT simulation of the adsorption of sodium silicate species on kaolinite surfaces. *Applied Surface Science*, **370**, 403–409.
- Hartman, P. (1973) Structure and morphology. Pp. 367–402 in: *Crystal Growth: An Introduction* (P. Hartman, editor). North-Holland Publ. Co., Amsterdam.
- He, L., Lin, F., Li, X., Sui, H., and Xu, Z. (2015) Interfacial sciences in unconventional petroleum production: From fundamentals to applications. *Chemical Society Reviews*, **44**, 5446–5494.
- Hohenberg, P. and Kohn, W. (1964) Inhomogeneous electron gas. *Physical Review*, **136**, 864–871.
- Kalinichev, A.G., Liu, X., and Cygan, R.T. (2016) Introduction to a special issue on molecular computer simulations of clays and clay-water interfaces: Recent progress, challenges, and opportunities. *Clays and Clay Minerals*, **64**, 335–336.
- Kohn, W. and Sham, L.J. (1965) Self-consistent equations including exchange and correlation effects. *Physical Review*, **140**, 1133–1138.
- Kremleva, A., Krüger, S., and Rösch, N. (2015) Uranyl adsorption at solvated edge surfaces of 2:1 smectites. A density functional study. *Physical Chemistry Chemical Physics*, **17**, 13757–13768.
- Kremleva, A. and Krüger, S. (2016) Comparative computational study of Np(V) and U(VI) adsorption on (110) edge surfaces of montmorillonite. *Clays and Clay Minerals*, **64**, 438–451.
- Kubicki, J.D., Schroeter, L.M., Itoh, M.J., Nguyen, B.N., and Apitz, S.E. (1999) Attenuated total reflectance Fourier-transform infrared spectroscopy of carboxylic acids adsorbed onto mineral surfaces. *Geochimica et Cosmochimica Acta*, **63**, 2709–2725.
- Lee, S.S., Fenter, P., Nagy, K.L., and Sturchio, N.C. (2012) Monovalent ion adsorption at the muscovite (001)-solution interface: Relationships among ion coverage and speciation, interfacial water structure, and substrate relaxation. *Langmuir*, **28**, 8637–8650.
- Lew, B.W., Wolfrom, M.L., and Max Goepf, Jr., R. (1946) Chromatography of sugars and related polyhydroxy compounds. *Journal of the American Chemical Society*, **68**, 1449–1453.
- Liu, X., Lu, X., Meijer, E.J., Wang, R., and Zhou, H. (2012a) Atomic-scale structures of interfaces between phyllosilicate edges and water. *Geochimica et Cosmochimica Acta*, **81**, 56–68.
- Liu, X., Meijer, E.J., Lu, X., and Wang, R. (2012b) First-principles molecular dynamics insight into Fe<sup>2+</sup> complexes adsorbed on edge surfaces of clay minerals. *Clays and Clay Minerals*, **60**, 341–347.
- Liu, X., Lu, X., Sprik, M., Cheng, J., Meijer, E.J., and Wang, R. (2013) Acidity of edge surface sites of montmorillonite and kaolinite. *Geochimica et Cosmochimica Acta*, **117**, 180–190.
- Liu, X., Cheng, J., Sprik, M., Lu, X., and Wang, R. (2014) Surface acidity of 2:1-type dioctahedral clay minerals from first principles molecular dynamics simulations. *Geochimica et Cosmochimica Acta*, **140**, 410–417.
- Łodziana, Z., Topsøe, N.-Y., and Nørskov, J.K. (2004) A negative surface energy for alumina. *Nature Materials*, **3**, 289–293.
- Martins, D.M.S., Molinari, M., Gonçalves, M.A., Mirão, J.P., and Parker, S.C. (2014) Toward modeling clay mineral nanoparticles: The edge surfaces of pyrophyllite and their interaction with water. *Journal of Physical Chemistry C*, **118**, 27308–27317.
- Mathur, A., Sharma, P., and Cammarata, R.C. (2005) Negative surface energy- clearing up confusion. *Nature Materials*, **4**, 186.
- Meunier, A. (2006) Why are clay minerals small? *Clay Minerals*, **41**, 551–566.
- Mohammed, M. and Babadagli, T. (2015) Wettability alteration: A comprehensive review of materials/methods and testing the selected ones on heavy-oil containing oil-wet systems. *Advances in Colloid and Interface Science*, **220**, 54–77.
- Monkhorst, H.J. and Pack, J.D. (1976) Special points for Brillouin-zone integrations. *Physical Review B*, **13**, 5188–5192.
- Morodome, S. and Kawamura, K. (2011) *In situ* X-ray diffraction study of the swelling of montmorillonite as

- affected by exchangeable cations and temperature. *Clays and Clay Minerals*, **59**, 165–175.
- Nakamura, Y., Yamagishi, A., Matumoto, S., Tohkubo, K., Ohtu, Y., and Yamaguchi, M. (1989) High-performance liquid chromatography for optical resolution on a column of an ion-exchange adduct of spherically shaped synthetic hectorite and optically active metal complexes. *Journal of Chromatography A*, **482**, 165–173.
- Newton, A.G. and Sposito, G. (2015) Molecular dynamics simulations of pyrophyllite edge surfaces: Structure, surface energies, and solvent accessibility. *Clays and Clay Minerals*, **63**, 277–289.
- Newton, A.G., Kwon, K.D., and Cheong, D. (2016) Edge structure of montmorillonite from atomistic simulations. *Minerals*, **6**, 25.
- Perdew, J.P., Burke, K., and Ernzerhof, M. (1996) Generalized gradient approximation made simple. *Physical Review Letters*, **77**, 3865–3868.
- Pintea, S., de Poel, W., de Jong, A.E.F., Vonk, V., van der Asdonk, P., Drnec, J., Balmes, O., Isern, H., Dufrane, T., Felici, R., and Vlieg, E. (2016) Solid–liquid interface structure of muscovite thin in CsCl and RbBr solutions. *Langmuir*, **32**, 12955–12965.
- Rappe, A.M., Rabe, K.M., Kaxiras, E., and Joannopoulos, J.D. (1990) Optimized pseudopotentials. *Physical Review B*, **41**, 1227–1230.
- Ray, S.S. (2014) Recent trends and future outlooks in the field of clay-containing polymer nanocomposites. *Macromolecular Chemistry and Physics*, **215**, 1162–1179.
- Sakuma, H. (2013) Adhesion energy between mica surfaces: Implications for the frictional coefficient under dry and wet conditions. *Journal of Geophysical Research: Solid Earth*, **118**, 6066–6075.
- Sakuma, H. (2015) Interlayer bonding energy of Mg-chlorite: A density functional theory study. *Journal of Computer Chemistry, Japan*, **14**, 152–154.
- Sakuma, H. and Suehara, S. (2015) Interlayer bonding energy of layered minerals: Implication for the relationship with friction coefficient. *Journal of Geophysical Research B: Solid Earth*, **120**, 2212–2219.
- Sakuma, H., Kondo, T., Nakao, H., Shiraki, K., and Kawamura, K. (2011) Structure of hydrated sodium ions and water molecules adsorbed on the mica / water interface. *The Journal of Physical Chemistry C*, **115**, 15959–15964.
- Schlegel, M.L., Nagy, K.L., Fenter, P., Cheng, L., Sturchio, N.C., and Jacobsen, S.D. (2006) Cation sorption on the muscovite (001) surface in chloride solutions using high-resolution X-ray reflectivity. *Geochimica et Cosmochimica Acta*, **70**, 3549–3565.
- Sun, B.N. and Baronnet, A. (1989a) Hydrothermal growth of OH-phlogopite single crystals I. Undoped growth medium. *Journal of Crystal Growth*, **96**, 265–276.
- Sun, B.N. and Baronnet, A. (1989b) Hydrothermal growth of OH-phlogopite single crystals. II. Role of Cr and Ti adsorption on crystal growth rates. *Chemical Geology*, **78**, 301–314.
- Tachi, Y. and Yotsuji, K. (2014) Diffusion and sorption of Cs<sup>+</sup>, Na<sup>+</sup>, I<sup>-</sup> and HTO in compacted sodium montmorillonite as a function of porewater salinity: Integrated sorption and diffusion model. *Geochimica et Cosmochimica Acta*, **132**, 75–93.
- Tansho, M., Tamura, K., and Shimizu, T. (2016) Identification of multiple Cs<sup>+</sup> adsorption sites in a hydroxy-interlayered vermiculite-like layered silicate through <sup>133</sup>Cs MAS NMR analysis. *Chemistry Letters*, **45**, 1385–1387.
- Tazi, S., Rotenberg, B., Salanne, M., Sprick, M., and Sulpizi, M. (2012) Absolute acidity of clay edge sites from *ab-initio* simulations. *Geochimica et Cosmochimica Acta*, **94**, 1–11.
- Tournassat, C., Ferrage, E., Poinssignon, C., and Charlet, L. (2004) The titration of clay minerals: II. Structure-based model and implications for clay reactivity. *Journal of Colloid and Interface Science*, **273**, 234–246.
- Tsipursky, S.I. and Drits, V.A. (1984) The distribution of octahedral cations in the 2:1 layers of dioctahedral smectites studied by oblique-texture electron diffraction. *Clay Minerals*, **19**, 177–193.
- Voorva, V.K., Al-Saidi, W.A., and Jordan, K.D. (2011) Density functional theory study of pyrophyllite and M-montmorillonites (M = Li, Na, K, Mg, and Ca): Role of dispersion interactions. *Journal of Physical Chemistry A*, **115**, 9695–9703.
- Welfare, H., Sposito, G., Skipper, N.T., Sutton, R., Park, S.-H., Soper, A.K., and Greathouse, J.A. (1999) Surface geochemistry of the clay minerals. *Proceedings of the National Academy of Sciences*, **96**, 3358–3364.
- White, G.N. and Zelazny, L.W. (1988) Analysis and implications of the edge structure of dioctahedral phyllosilicates. *Clays and Clay Minerals*, **36**, 141–146.
- Yamagishi, A. and Sato, H. (2012) Stereochemistry and molecular recognition on the surface of a smectite clay mineral. *Clays and Clay Minerals*, **60**, 411–419.
- Zhang, C., Liu, X., Lu, X., Meijer, E.J., Wang, K., He, M., and Wang, R. (2016) Cadmium(II) complexes adsorbed on clay edge surfaces: Insight from first principles molecular dynamics simulation. *Clays and Clay Minerals*, **64**, 337–347.

(Received 06 March 2017; revised 14 July 2017; Ms. 1168; AE: X. Liu)